Int. J. Electrochem. Sci., 17 **(2022)** Article Number: 220962, doi: 10.20964/2022.09.59

International Journal of
ELECTROCHEMICAL
SCIENCE
www.electrochemsci.org

Electro-oxidation of Quinoline Simulated Wastewater Containing Chloride in a Swirling Flow Reactor: Influence Factors, Kinetics, Biotoxicity, and Energy Consumption

Haiyan Li[1,2], Enkai Fu[1], Chunrong Wang[1,], Lei He[1], Xiaoya Chen[1], Shu Ke[1], Mingchuan Zhao[1], Rongfei Feng[1], Yang Li[1]*

[1] School of Chemical and Environmental Engineering, China University of Mining and Technology (Beijing), Beijing, 100083, PR China
[2] School of Civil and Architectural Engineering, Guizhou University of Engineering Science, Bijie, 551700, PR China
[*]E-mail: wcr@cumtb.edu.cn

Received: 1 June 2022 / *Accepted:* 18 July 2022 / *Published:* 7 August 2022

In this research, we used a swirling flow reactor to remove quinoline from aqueous solutions containing chloride using electro-oxidation (EO). We evaluated the effect of several operational variables, including current density, initial pH, Cl^- concentration, and initial quinoline concentration, on EO effectiveness. Our results revealed a maximum total organic carbon (TOC) removal efficiency of 68.0% at a current density of 40 mA cm^{-2}, Cl^- concentration of 2000 mg L^{-1}, and initial quinoline concentration of 250 mg L^{-1}. Of the variables tested, current density had the largest effect on TOC abatement. Kinetic analysis showed that quinoline abatement followed pseudo-first-order kinetics and was limited by charge transfer. The biotoxicity of quinoline simulated wastewater increased and then decreased during EO. Energy consumption and mineralization current efficiency during 90 min of electrolysis in the swirling flow reactor were 1.67 kWh (g TOC)$^{-1}$ and 8.1%, respectively, indicating superior performance compared to the parallel plate reactor. This paper provides information on developing electrochemical reactors and their application to reduce the organic load of saline wastewater.

Keywords: Quinoline; Electro-oxidation; Biotoxicity; Energy consumption; Swirling flow reactor

1. INTRODUCTION

Quinoline is used as raw material and solvent for the manufacture of dyes, paints, herbicides, and other fine chemicals [1]. It is widely existed in coal coking wastewater [2], coal gasification wastewater [3], pharmaceutical wastewater, and pulping wastewater [4]. Quinoline is classified as a priority pollutant by the United States Environmental Protection Agency owing to its toxicity, carcinogenicity,

and teratogenicity [5]. Biological treatment has a limited ability to remove quinoline from wastewater [6, 7], and therefore alternative methods are urgently needed to reduce ecological harm.

Electro-oxidation (EO) is a new advanced oxidation technology that has attracted wide attention for its use in the degradation of refractory organic compounds [8, 9, 10]. EO has several benefits, including simple process control, stable performance, environmental friendliness, and no additional chemical reagents. The plate reactor is currently the predominant type of reactor, but it has many shortcomings in practical applications, such as poor mass transfer and high energy consumption [11, 12]. Simulations and laboratory experiments have confirmed that swirling flow in an electrochemical reactor could enhance mass transfer [13, 14]. For example, a rotating multi-electrodes reactor increased the phenol degradation rate by 1.45 times, and the mass transfer coefficient increased by 110%. The rotating anode increased liquid disturbance and reduced the residence time of the bubble curtain [15]. A cyclone electrochemical reactor was designed for simultaneous degradation of phenol and metal recovery, with a current efficiency of 90.3% [16]. Research on swirling flow reactors has mainly focused on the indirect oxidation of hydroxyl radicals, and relatively little work has been conducted on active chlorine-mediated electrochemical oxidation.

Cl^- is a pervasive halide ion in almost all water matrices. Since the potential of chlorine evolution is lower than that of oxygen evolution, the chlorine evolution reaction occurs preferentially [17, 18]. Active chlorine, Cl_2 (E^0 = 1.36 V/SHE)/HClO (E^0 = 1.49 V/SHE)/ClO^- (E^0 = 0.89 V/SHE), plays a major role in EO [19]. Unlike the direct injection of chlorine gas, active chlorine generated in situ does not require the addition of any chemical reagents and avoids secondary pollution. Additionally, the Ti/RuO_2-IrO_2 anode has several characteristics that make it ideal for this application: low chlorine evolution potential, comparably large removal efficiency, low energy consumption, and suitability when treating high-salinity reverse osmosis concentrate [17].

To study the application of swirling flow reactors in EO, we tested their ability to treat quinoline simulated wastewater containing chloride. We first evaluated how current density, Cl^- concentration, pH, and initial quinoline concentration affect quinoline and TOC removal efficiency. To identify which variable has the strongest effect on EO, we designed an orthogonal experiment informed by the results of the single variable experiments. We then analyzed quinoline degradation kinetics and biotoxicity during EO. Finally, we compared energy consumption (EC) and mineralization current efficiency (MCE) of the swirling flow reactor and the parallel plate reactor. This study will improve the development of electrochemical reactors and explore their potential applications.

2. MATERIALS AND METHODS

2.1 Chemicals and reagents

Chromatographic grade quinoline and methanol (99.9%) were obtained from Tianjin jinke Fine Chemical Research Institute (Tianjin, China), and all the other chemicals (e.g., NaCl, NaOH, and H_2SO_4) were of analytical grade and were purchased from Sinopharm Chemical Reagent Co., Ltd. (Beijing, China). All chemicals were used directly without further purification. All solutions were prepared with

deionized water.

2.2 Experimental setup

The process diagrams of our experimental system and the picture of our swirling flow reactor are shown in Figure 1. The swirling flow reactor unit used in this study was of 240 mL capacity and made of polymethyl methacrylate (Figure 1b). The swirling flow reactor comprised one anode (Φ38 mm, 1 mm thick) and two cathode electrodes (Φ60 mm, 1 mm thick; Φ16 mm cylinder). The electrodes were vertically installed inside the electrolytic cell and the anode was placed between the two cathode electrodes with an inter-electrode gap of 10 mm. The Ti/RuO_2-IrO_2 anode and pure titanium cathode electrodes were supplied by Henan Hengli Titanium Equipment Manufacturing Co., Ltd (Luohe, China). The effective anode active geometric area was 225 cm^2. The influent flowed tangentially into the outer channel of the reactor. 500 mL of simulated wastewater were treated per batch experiment unless otherwise stated. To compare the performance of different reactors, electrodes of equal size (150×150×1.5 mm) were inserted vertically in the plate reactor. The current was controlled using a DC power supply (Hongshengfeng, DPS-305BF). Based on previous results from our group, we varied the current density from 10 mA cm^{-2} to 50 mA cm^{-2}. The concentration of quinoline was equivalent to that in coal chemical wastewater [2]. The flow rate between the electrochemical cell and reservoir was set to 320 mL min^{-1} and controlled by a peristaltic pump (LongerPump, BT100-2J). All samples were collected from the reservoir tank.

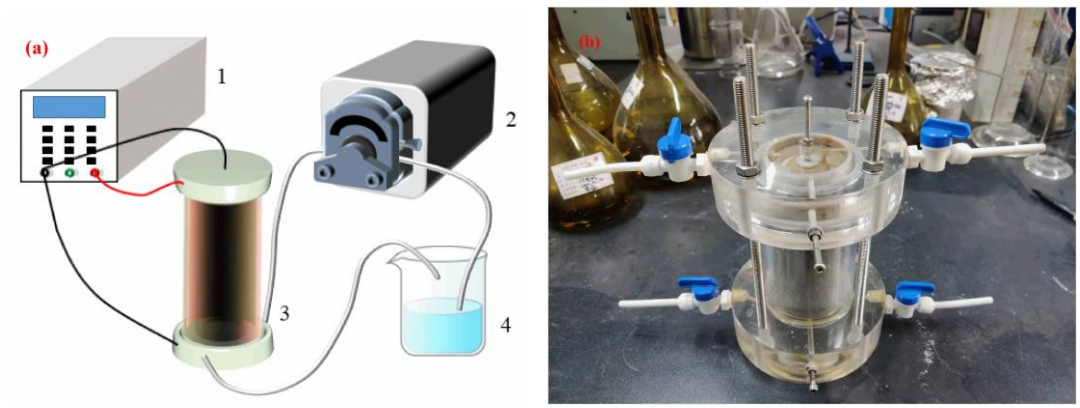

Figure 1. The process diagram of experimental system (a) (1: DC power supply, 2: peristaltic pump, 3: swirling flow reactor, 4: reservoir tank.), and the photograph of the swirling flow reactor (b).

2.3 Analytical methods

All samples were taken with syringes and filtered through a 0.45 μm PTFE filter (Whatman) before analysis. The concentration of quinoline in each aqueous solution was analyzed by high-performance liquid chromatography (HPLC, LC-10AT, Shimadzu, Japan) equipped with a SPD10A UV-Vis Detector. The chromatographic column was Wondasil TM C18 (5 μm, 4.6 × 150 mm). Detection

wavelength was 275 nm. The mobility was methanol: water =80:20 with a flow rate of 0.7 ml min^{-1}, and the injection volume was 2 μL. The concentration of total organic carbon (TOC) was measured with a TOC analyzer (TOC-L CPH, Shimadzu, Japan). Biotoxicity analysis was carried out using a luminescent bacteria inhibition test according to prevailing Chinese standards (GB/T 15441-1995, Water quality-Determination of the acute toxicity-Luminescent bacteria test). The freeze-dried powder of the luminescent bacterium *Photobacterium phosphoreum T3 spp.* was obtained from Nanjing Institute of Soil Science, Chinese Academy of Sciences.

The EC for treated per gram TOC was calculated by equation (1) [20]:

$$\mathrm{EC\ (kWh\ (g\ TOC)^{-1})} = \frac{\mathrm{UIt}}{(\Delta \mathrm{TOC})\mathrm{V}} \qquad (1)$$

Where U, I, V, t, and ΔTOC represent the average potential difference of the cell (V), applied current (A), solution volume (0.5 L), electrolysis time (h), and the experimental TOC decay (mg L^{-1}), respectively.

Quinoline mineralization was assessed from the decay of TOC. The MCE for the treated solutions can be calculated from equation (2) [20]:

$$\mathrm{MCE} = \frac{(\Delta \mathrm{TOC})\mathrm{nFV}}{4.32\times10^{7}\mathrm{mIt}} \times 100\% \qquad (2)$$

Where n is the number of electrons exchanged per organic molecule during the mineralization process (48), F is the Faraday constant (96487 C mol^{-1}) and m is the number of carbon atoms in the molecule (9). The quinoline mineralization reaction can be represented as follows:

$$C_9H_7N + 21H_2O \rightarrow 9CO_2 + 49H^+ + NO_3^- + 48e^- \qquad (3)$$

3. RESULTS AND DISCUSSION

3.1 Effects of operating parameters on EO effectiveness

3.1.1 Effect of current density

We examined effect of current density on quinoline and TOC abatement and discovered that quinoline concentration decreased with operation time when a current was applied (Figure 2a). Quinoline removal efficiency also increased with the increase of current density. When the current density was 10, 20, 30, 40, and 50 mA cm^{-2}, quinoline removal efficiencies after 90 min were 60.7%, 73.1%, 87.7 %, 95.8%, and 100%, respectively. A similar trend can be observed in the removal of TOC. When the current density was 50 mA cm^{-2}, the TOC removal efficiency reached a maximum of 48.7 % (Figure 2b). Increase the current enhanced mineralization efficiency of quinoline. Higher current densities lead to higher removal efficiencies because of the greater driving force to accelerate pollutant oxidation. However, increasing current density led to an increased voltage between the plates. This, in turn, increased the side reaction of oxygen evolution on the anode, ultimately resulting in high energy consumption. The bubbles generated by the oxygen evolution reaction also adhered to the surface of the electrode, affecting the effective anode area of electrochemical oxidation [21]. Moreover, when the current density is too high, it will damage electrode morphology resulting in shortened service life [22].

After considering the impacts on quinoline removal efficiency and energy consumption, we chose 40 mA cm^{-2} for subsequent experiments.

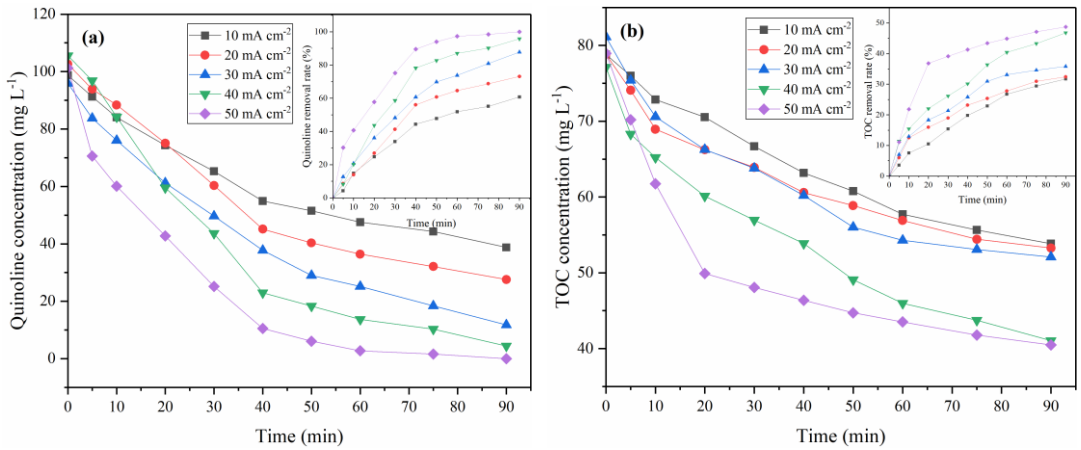

Figure 2. Effect of current density on (a) quinoline and (b) TOC removal. Conditions: [Cl^-] = 4000 mg L^{-1}, [quinoline] = 100 mg L^{-1}, without adjustment of initial pH. Insets show the quinoline/TOC removal rate.

3.1.2 Effect of Cl^- concentration

We next examined how varying the Cl^- concentration affects the effectiveness of EO in treating quinoline simulated wastewater. The quinoline removal efficiencies at Cl^- concentration of 1000, 2000, 3000, 4000, and 5000 mg L^{-1} were 97.6%, 100%, 98.7%, 95.8%, and 95.6%, respectively (Figure 3a). The highest quinoline removal efficiency was achieved when the Cl^- concentration was 2000 mg/L. At Cl^- concentration of 2000 mg L^{-1}, the TOC removal efficiency reached the maximum of 62.8%, while at high Cl^- concentration, the degree of quinoline mineralization by electrolysis was poor (Figure 3b). Studies have shown that adding more Cl^- can achieve higher removal efficiency of chemical oxygen demand in the electrochemical oxidation treatment of landfill leachate [23, 24]. High Cl^- concentration is conducive to the formation of active chlorine and reduced the cell voltage. However, it did not improve the removal efficiency of organic matter and instead increased the formation of undesired byproducts such as chlorates and perchlorates (equation (4-5)) [25]. Informed by our previous results regarding removal efficiency and by-product generation, we decided to use 2000 mg L^{-1} chloride for subsequent investigations.

$$Cl^- + 3H_2O \rightarrow ClO_3^- + 6H^+ + 6e^- \quad (4)$$

$$ClO_3^- + H_2O \rightarrow ClO_4^- + 2H^+ + 2e^- \quad (5)$$

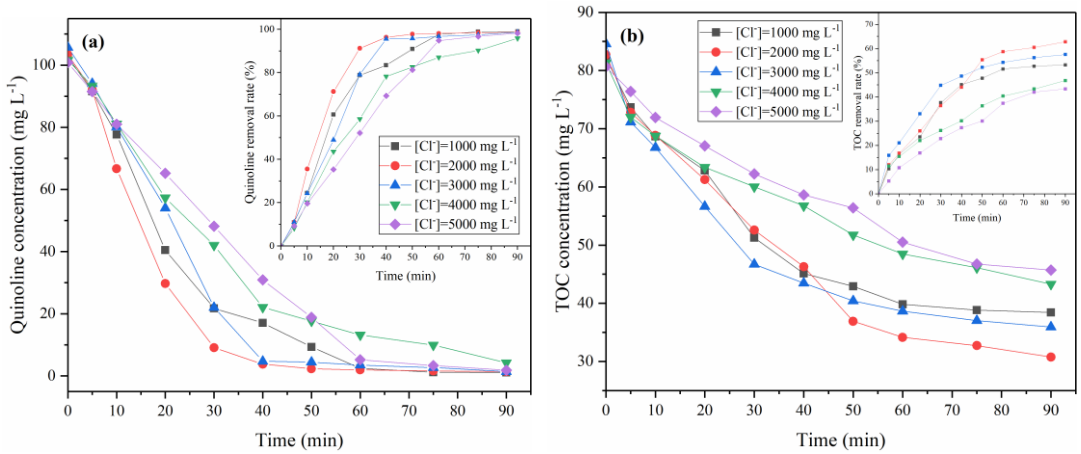

Figure 3. Effect of Cl^- concentration density on (a) quinoline and (b) TOC removal. Conditions: current density = 40 mA cm^{-2}, [quinoline] = 100 mg L^{-1}, without adjustment of initial pH. Insets show the quinoline/TOC removal rate.

3.1.3 Effect of pH

We then analyzed the effect of pH on electro-oxidation of quinoline simulated wastewater and found that acidic conditions were favorable for quinoline abatement. At pH 3, quinoline was removed within 20 min (Figure 4a). Due to the addition of acid or alkali to adjust pH, the quinoline was eventually removed at all pH conditions. HOCl is the predominant chlorine species in acidic conditions, while according to the fraction of aqueous active chlorine species as a function of pH, OCl^- predominates at pH values higher than 7.5 [26]. HOCl has a stronger oxidation ability than OCl^-. At pH 3, 5, 7, 9, and 11, the TOC removal efficiencies were 61.5%, 54.8%, 52.7%, 55.1%, and 58.5%, respectively (Figure 4b). Overall, acidic conditions are favorable for organic mineralization during EO of wastewater containing chloride.

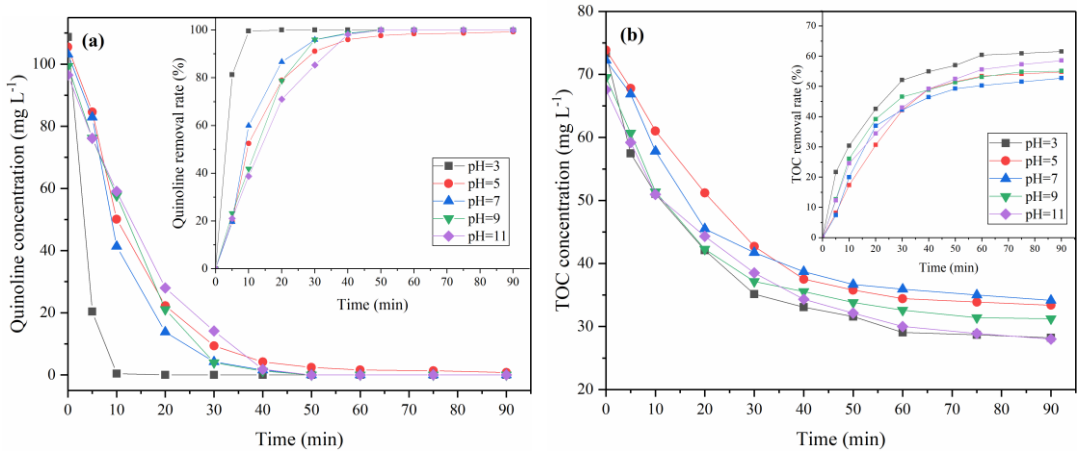

Figure 4. Effect of pH on (a) quinoline and (b) TOC removal. Conditions: current density = 40 mA cm^{-2}, [Cl^-] = 2000 mg L^{-1}, [quinoline] = 100 mg L^{-1}. Insets show the quinoline/TOC removal rate.

3.1.4 Effect of initial quinoline concentration

Then, we studied the removal of quinoline and TOC during EO at different initial quinoline concentrations. When current density was maintained at 40 mA cm^{-2} and initial quinoline concentrations were 50, 100, and 150 mg L^{-1}, quinoline was removed within 50, 75, and 90 min, respectively (Figure 5a). At higher initial quinoline concentrations of 200 and 250 mg L^{-1}, quinoline removal efficiencies were 99.5% and 98.6%, respectively. Quinoline was quickly removed at low initial quinoline concentrations. In the swirling flow reactor, sufficient active chlorine was generated by electrolysis, resulting in the reduction of quinoline. Figure 5b shows the degree of quinoline mineralization by electrolysis in the swirling flow reactor at different initial quinoline concentrations. With the increase of initial quinoline concentration from 50mg L^{-1} to 250mg L^{-1}, TOC removal efficiency increased from 51.9% to 66.6% in 90 min. This can be ascribed to the fact that the high concentration of quinoline enabled improved utilization efficiency of active chlorine. By increasing the possibility of the intermediate product being attacked by an oxidant. When the initial quinoline concentration was greater than 200 mg L^{-1}, the TOC removal efficiency changed little. One possible explanation is that quinoline degradation intermediates cannot be further oxidized in this system or the yield of oxidants such as active chlorine was insufficient.

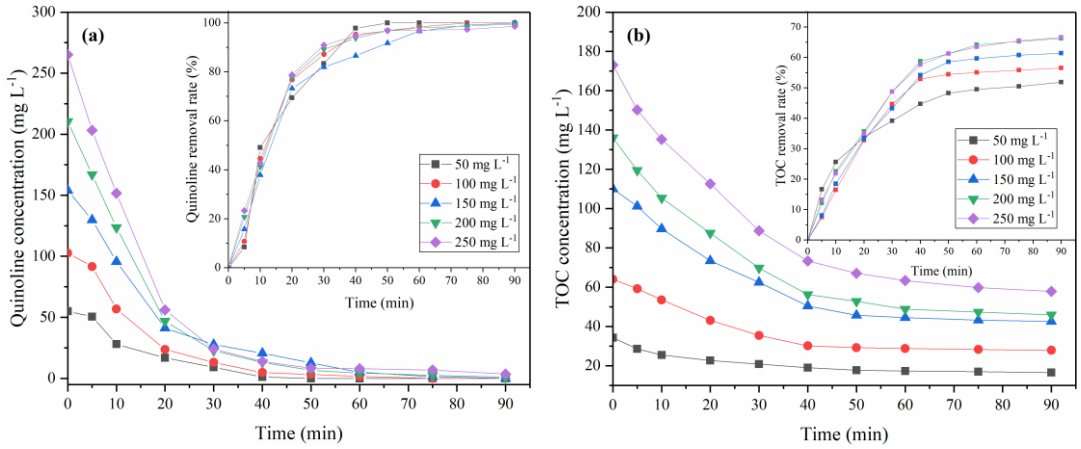

Figure 5. Effect of initial quinoline concentration on (a) quinoline and (b) TOC removal. Conditions: current density = 40 mA cm^{-2}, $[Cl^-]$ = 2000 mg L^{-1}, without adjustment of initial pH. Insets show the quinoline/TOC removal rate.

3.1.5 Orthogonal experiment

To further explore the influence of operating conditions on the EO of quinoline by the Ti/RuO_2-IrO_2 anode in a swirling flow reactor, we conducted an orthogonal experiment in which we measured how a subset of our operating variables affected TOC removal during EO. Based on the results of our single factor experiments, we chose to exclude pH and instead focus on current density, Cl^- concentration, and initial quinoline concentration. The factor levels are shown in Table 1.

Table 1. Factors and levels of influencing factors in EO.

Level	Factors		
	Current density (mA cm^{-2})	Cl^- concentration (mg L^{-1})	Initial quinoline concentration (mg L^{-1})
1	30	1000	150
2	40	2000	200
3	50	3000	250

Usually, the range analysis method is used for orthogonal experiment analysis. R_j denotes the range, which is the difference between the maximum and minimum mean values at the level of the j column. The corresponding calculation formula is as follows:

$$R_j = \max(k_{1j}, k_{2j}, \ldots k_{ij}) - \min(k_{1j}, k_{2j}, \ldots k_{ij}) \quad (6)$$

Where k_{ij} denotes the sum of experimental data corresponding to the level i of the factor under column j. The larger the calculated R_j, the greater the influence of the factor change on the test results. Therefore, the dominant factor of the testing level can be determined by the measurement results [27].

Following the above orthogonal list, 9 groups of experiments were used to investigate the TOC removal efficiency under various factors. The ranking ranges of the orthogonal results are shown in Table 2, where K_i represents the sum of all TOC removal efficiencies for a given factor at Level i. Table 2 shows that the relative importance of the three factors followed the order of A (current density) > B (Cl^- concentration) > C (initial quinoline concentration). Therefore, current density should be given priority when analyzing the effects of multiple influencing factors in practical application. TOC removal efficiency reached its maximum at 40 mA cm^{-2} current density, 2000 mg L^{-1} Cl^- concentration, 250 mg L^{-1} quinoline concentration (A2B2C3).

Table 2. Orthogonal experiment arrangement and the corresponding result analysis.

	Current density (mA cm^{-2})	Cl^- concentration (mg L^{-1})	Initial quinoline concentration (mg L^{-1})	TOC removal efficiency (%)
1	30	1000	150	46.6
2	30	2000	200	56.9
3	30	3000	250	55.9
4	40	1000	200	59.7
5	40	2000	250	68.0
6	40	3000	150	60.5
7	50	1000	250	65.3
8	50	2000	150	67.1
9	50	3000	200	67.2
K_1	159.4	171.6	174.2	
K_2	188.2	192.0	183.8	
K_3	199.6	183.6	189.2	
Range (R_j)	40.2	20.4	15.0	
Significance of factors	A>B>C			
Optimal parameter	A2B2C3			

3.2 Kinetics analysis of quinoline degradation

Pseudo-first-order kinetics (Table 3) were observed in the EO of quinoline simulated wastewater containing chloride, and the variance R^2 of the fitting equation was greater than 91%. When the current density increased from 10 mA cm^{-2} to 50 mA cm^{-2}, the apparent rate constant (k_{app}) rose from 0.010 min^{-1} to 0.058 min^{-1}. A linear relationship was found between the degradation rate of quinoline and the applied current (Figure 6). Similar results were obtained in other studies [28, 29]. As current density increased, active chlorine was produced at a higher rate increased when electrolysis of the solution contained a high concentration of chloride ions, and k_{app} also increased linearly with current density.

When Cl^- concentration reached 2000 mg L^{-1}, k_{app} reached its maximum value of 0.064 min^{-1}, but the quinoline degradation rate did not change significantly at high Cl^- concentration. Many studies have shown that increasing chloride concentration is beneficial for electrochemical oxidation of organics [30, 31, 32]; however, this was not shown in our study. We speculate that the concentration of active chlorine and oxidizing species fluctuated slightly at this current density and Cl^- concentration range.

Due to the addition of acid or alkali to adjust pH, k_{app} was higher than that of other groups. At pH 3, k_{app} reached its maximum value of 0.552 min^{-1}. Hypochlorous acid is a stronger oxidant than hypochlorite and takes a dominant role at pH ranging from 3.0 to 7.5 [33], which explains why the system has poor performance in neutral and alkaline conditions.

EO is controlled by both charge and mass transfer [34]. When the initial quinoline concentration increased from 50 to 250 mg L^{-1}, k_{app} increased and then decreased, indicating that mass transfer limitation was not the main reason for the initial quinoline increase. Instead, our results suggest that the degradation of quinoline was primarily controlled by charge transfer.

Table 3. Electrochemical degradation kinetics of quinoline at different initial conditions.

Parameters		k_{app} (min^{-1})	$t_{1/2}$ (min)	R^2	Quinoline removal efficiency
Current density (mA cm^{-2})	10	0.010	59.9	0.97	60.7%
	20	0.015	41.7	0.97	73.1%
	30	0.023	30.3	0.99	87.7%
	40	0.035	21.8	0.99	95.8%
	50	0.058	13.4	0.99	100%
Cl^- concentration (mg L^{-1})	1000	0.058	15.5	0.96	97.6%
	2000	0.064	9.4	0.93	100%
	3000	0.058	13.4	0.92	98.7%
	4000	0.035	21.8	0.99	95.8%
	5000	0.048	21.6	0.96	95.6%
pH	3	0.552	1.9	0.95	100%
	5	0.079	9.3	0.99	99.3%
	7	0.110	7.8	0.99	100%
	9	0.114	9	0.98	100%
	11	0.093	10.8	0.92	100%
Initial quinoline concentration (mg L^{-1})	50	0.062	12.1	0.98	100%
	100	0.074	10.8	0.99	100%
	150	0.054	12.9	0.98	100%
	200	0.062	9.5	0.98	99.5%
	250	0.049	5.9	0.91	98.6%

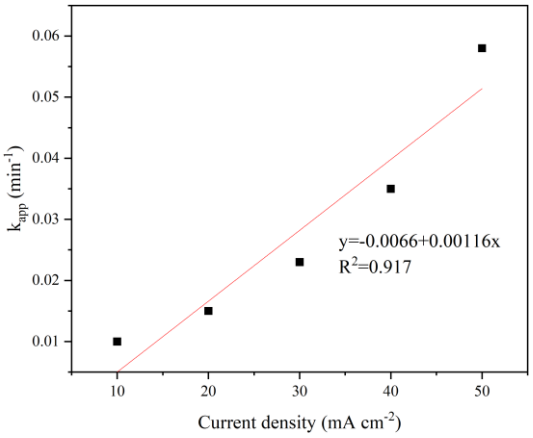

Figure 6. Apparent rate constant (k_{app}) of quinoline degradation at different current densities.

3.3 Biological toxicity analysis

The 15 min acute toxicity tests were carried out on quinoline simulated wastewater during EO. The inhibition rate of the luminescent bacterium increased from 83.4% to 96.1% and then decreased to 40.1% (Figure 7). The increase in inhibition rate indicated that the intermediate product produced in the reaction was more toxic than quinoline. A similar result was observed in other studies and was attributed to the production of highly toxic chlorinated by-products [35].

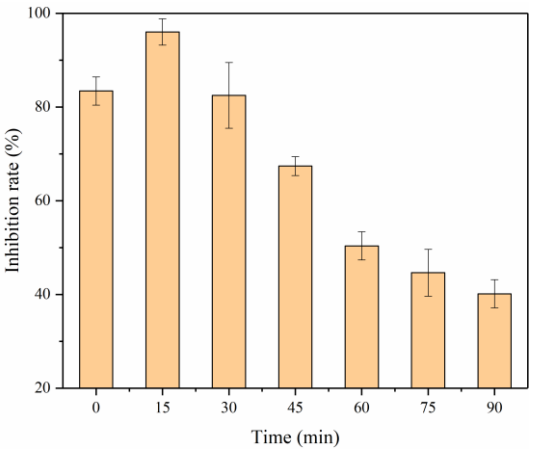

Figure 7. Inhibition rate of the luminescent bacterium during EO. Conditions: current density = 40 mA cm^{-2}, [Cl^-] = 2000 mg L^{-1}, [quinoline] = 250 mg L^{-1}, without adjustment of initial pH.

3.4 Energy consumption and mineralization current efficiency

3.4.1 Comparison of EC between plate reactor and swirling flow reactor

The EC for EO of quinoline was compared between the parallel plate reactor and swirling flow reactor (Figure 8). In both reactors, the energy consumption per gram of TOC removal increased with

reaction time. The EC for 500 mL of quinoline simulated wastewater with an electrolytic time of 90 min at a current density of 40 mA cm^{-2} was 1.67 kWh (g TOC)$^{-1}$ in the swirling flow reactor compared to 2.00 kWh (g TOC)$^{-1}$ for parallel plate reactor. The EC in the swirling flow reactor was lower than that of the parallel plate reactor, indicating that the turbulent flow in the swirling flow reactor increased the mass transfer and improved the degradation of organic matter.

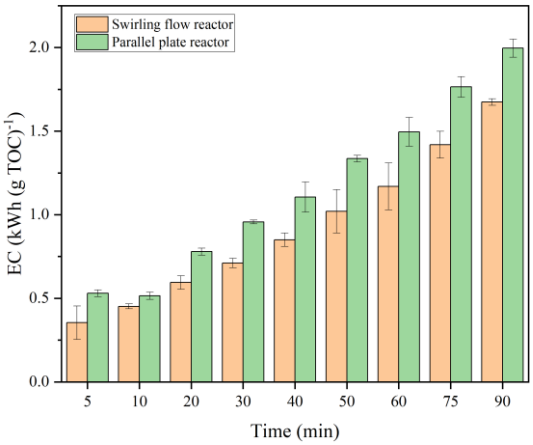

Figure 8. EC during EO of quinoline in the swirling flow reactor. Conditions: current density = 40 mA cm^{-2}, [Cl^-] = 2000 mg L^{-1}, [quinoline] = 250 mg L^{-1}, without adjustment of initial pH.

3.4.2 Comparison of MCE between plate reactor and swirling flow reactor

MCE during EO was compared between the parallel plate reactor and the swirling flow reactor (Figure 9). In both reactors, MCE decreased with reaction time. In the parallel plate reactor, MCE decreased from 25.6 % to 6.8 % in 90 min and from 38.3 to 8.1% in the swirling flow reactor.

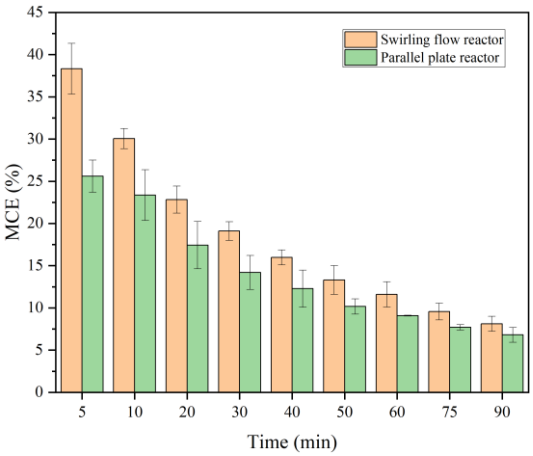

Figure 9. MCE during EO of quinoline in the swirling flow reactor. Conditions: current density = 40 mA cm^{-2}, [Cl^-] = 2000 mg L^{-1}, [quinoline] = 250 mg L^{-1}, without adjustment of initial pH.

The limited mass transfer caused more loss of electric energy in the form of side reactions and heat production, resulting in low current efficiency. This is a typical trend in electrochemical mass transfer-controlled processes [28, 36, 37]. MCE in the swirling flow reactor was higher than in the parallel plate reactor, indicating that the formation of swirl flow in the reactor is beneficial to mass transfer.

4. CONCLUSIONS

In this study, we investigated how operational variables influence the effectiveness of EO in removing quinoline from chloride-containing wastewater in a swirling flow reactor. We also examined kinetics, biotoxicity, and energy consumption during EO and compared the performance of swirling flow reactors to that of plate reactors. The removal efficiency of quinoline and TOC increased gradually with the increase of current density. Increasing Cl^- concentration improved the removal efficiency of quinoline, but only up to point, beyond which adding more Cl^- promoted the side reaction and was not conducive to the degradation of organic matter. Acidic conditions were generally favorable for quinoline degradation and mineralization. The quinoline removal efficiencies were comparable under different initial quinoline concentrations. Quinoline degradation in the swirling flow reactor followed pseudo-first-order reaction kinetics. The k_{app} of quinoline degradation increased from 0.010 min^{-1} to 0.058 min^{-1} linearly as current density increased. All k_{app} were higher than other groups due to the addition of acid or alkali to adjust pH. The k_{app} analysis showed that the degradation of quinoline in the swirling flow reactor was limited by electron transfer. To determine which variable had the strongest effect on TOC removal, we conducted an orthogonal experiment, which showed that the order of the effect on TOC removal was: current density > Cl^- concentration > initial quinoline concentration. The TOC removal efficiency reached its maximum value of 68.0% at a current density of 40 mA cm^{-2}, 2000 mg L^{-1} Cl^- concentration, and 250 mg L^{-1} initial quinoline concentration. The biotoxicity of quinoline simulated wastewater started at 83.4% inhibition, increased to 96% inhibition, and then decreased to 40.1% inhibition during EO. We found that for an electrolytic time of 90 min and a current density of 40 mA cm^{-2}, EC and MCE were 1.67 kWh $(g\ TOC)^{-1}$ and 8.1%, respectively. Tangential inflow in the swirling flow reactor promoted turbulence and mass transfer, resulting in lower energy consumption compared to the parallel plate reactor. The results provided a theoretical basis for the development of electrochemical reactors and the engineering application of EO.

ACKNOWLEDGMENTS
The authors gratefully acknowledge the support from the National Natural Science Foundation of China (No. 51978658) and Guizhou Provincial Department of Education Youth Science and Technology Talents Growth Project (No. KY [2022]127).

References

1. J. Jing, W. Li, A. Boyd, Y. Zhang, V. L. Colvin, W. W. Yu, *J. Hazard. Mater.*, 237-238 (2012) 247.
2. D. Liu, C. Wang, Y. Song, Y. Wei, L. He, B. Lan, X. He, J. Wang, *Chemosphere*, 227 (2019) 647.
3. C. Wang, K. Ma, T. Wu, M. Ye, P. Tan, K. Yan, *Chemosphere*, 149 (2016) 219.

4. K. V. Padoley, S. N. Mudliar, R. A. Pandey, *Bioresour. Technol.*, 99 (2008) 4029.
5. L. Chu, S. Yu, J. Wang, *Radiat Phys. Chem.*, 144 (2018) 322.
6. C. Wang, M. Zhang, F. Cheng, Q. Geng, *Biosci Biotechnol. Biochem*, 79 (2015) 164.
7. X. Wu, X. Wu, J. Li, Q. Wu, Y. Ma, W. Sui, L. Zhao, X. Zhang, *Msphere*, 5 (2020) e00246.
8. L. He, C. Wang, X. Chen, L. Jiang, Y. Ji, H. Li, Y. Liu, J. Wang, *Chemosphere*, 288 (2022) 132362.
9. C. Wang, M. Zhang, M. Ye, J. Wang, G. Li, *J. Chem. Technol. Biotechnol.*, 89 (2014) 1599.
10. S. Garcia-Segura, X. Qu, P. J. J. Alvarez, B. P. Chaplin, W. Chen, J. C. Crittenden, Y. Feng, G. Gao, Z. He, C.-H. Hou, X. Hu, G. Jiang, J.-H. Kim, J. Li, Q. Li, J. Ma, J. Ma, A. B. Nienhauser, J. Niu, B. Pan, X. Quan, F. Ronzani, D. Villagran, T. D. Waite, W. S. Walker, C. Wang, M. S. Wong, P. Westerhoff, *Environ. Sci-Nano*, 7 (2020) 2178.
11. F. F. Rivera, T. Pérez, L. F. Castañeda, J. L. Nava, *Chem. Eng. Sci.*, 239 (2021) 116622.
12. Y. Zhang, K. Wei, W. Han, X. Sun, J. Li, J. Shen, L. Wang, *Electrochim. Acta*, 189 (2016) 1.
13. C. C. Contigiani, O. G. Perez, J. M. Bisang, *Chem. Eng. J.*, 350 (2018) 233.
14. C. C. Contigiani, J. P. Fornés, O. González Pérez, J. M. Bisang, *Chem. Eng. Process*, 157 (2020) 108111.
15. T. X. Fan, Y. Cai, G. W. Chu, Y. Luo, L. L. Zhang, J. F. Chen, *Ind. Eng. Chem. Res.*, 58 (2019) 2396.
16. M. Q. Hu, Z. Sun, J. G. Hu, H. Lei, W. Jin, *Ind. Eng. Chem. Res.*, 58 (2019) 12642.
17. M. Zhou, L. Liu, Y. Jiao, Q. Wang, Q. Tan, *Desalination*, 277 (2011) 201.
18. M. Panizza, G. Cerisola, *Chem. Rev.*, 109 (2009) 6541.
19. D. Rajkumar, J. G. Kim, *J. Hazard Mater.*, 136 (2006) 203.
20. E. Brillas, C. A. Martínez-Huitle, *Appl. Catal. B-Environ.*, 166 (2015) 603.
21. O. Scialdone, C. Guarisco, A. Galia, *Electrochim. Acta*, 58 (2011) 463.
22. M. Moradi, Y. Vasseghian, A. Khataee, M. Kobya, H. Arabzade, E.-N. Dragoi, *Journal of Industrial and Engineering Chemistry*, 87 (2020) 18.
23. Y. Deng, J. D. Englehardt, *Waste Manage*, 27 (2007) 380.
24. L.-C. Chiang, J.-E. Chang, T.-C. Wen, *Water Res.*, 29 (1995) 671.
25. P. Aravind, H. Selvaraj, S. Ferro, G. M. Neelavannan, M. Sundaram, *J. Clean. Prod.*, 182 (2018) 246.
26. A. E. Yañez-Rios, J. E. Carrera-Crespo, R. M. Luna-Sanchez, R. E. Palma-Goyes, J. Vazquez-Arenas, *J. Environ. Chem. Eng.*, 8 (2020) 104357.
27. Y. Wu, H. Zhao, C. Zhang, L. Wang, J. Han, *Energy*, 151 (2018) 79.
28. F. Zaviska, P. Drogui, J.-F. Blais, G. Mercier, *J. Appl. Electrochem.*, 39 (2009) 2397.
29. S. Kim, T.-H. Kim, C. Park, E.-B. Shin, *Desalination*, 155 (2003) 49.
30. C. Zhang, D. He, J. Ma, T. D. Waite, *Water Res.*, 145 (2018) 220.
31. R. V. McQuillan, G. W. Stevens, K. A. Mumford, *J. Hazard. Mater.*, 383 (2020) 121244.
32. S. Cotillas, J. Llanos, P. Canizares, D. Clematis, G. Cerisola, M. A. Rodrigo, M. Panizza, *Electrochim. Acta*, 263 (2018) 1.
33. I. M. D. Gonzaga, A. R. Dória, V. M. Vasconcelos, F. M. Souza, M. C. dos Santos, P. Hammer, M. A. Rodrigo, K. I. B. Eguiluz, G. R. Salazar-Banda, *J. Electroanal. Chem.*, 874 (2020) 114460.
34. H. Qin, X. Wei, Z. Ye, X. Liu, S. Mao, *Environ. Sci. Technol.*, 56 (2022) 5753.
35. M. Chen, X. Zhao, C. Wang, S. Pan, C. Zhang, Y. Wang, *J. Hazard. Mater.*, 401 (2021) 123295.
36. A. M. Polcaro, M. Mascia, S. Palmas, A. Vacca, *Ind. Eng. Chem. Res.*, 41 (2002) 2874.
37. G. Huang, J. Yao, W. Pan, J. Wang, *Environ. Sci. Pollut. Res.*, 23 (2016) 18288.